AIP | Review of Scientific Instruments

Miniature fiber-optic refractometer for measurement of salinity in double-diffusive thermohaline systems

T. L. Bergman, F. P. Incropera, and W. H. Stevenson

Citation: Review of Scientific Instruments **56**, 291 (1985); doi: 10.1063/1.1138346
View online: http://dx.doi.org/10.1063/1.1138346
View Table of Contents: http://scitation.aip.org/content/aip/journal/rsi/56/2?ver=pdfcov
Published by the AIP Publishing

Articles you may be interested in

Asymmetric Rayleigh-Taylor and double-diffusive fingers in reactive systems
Phys. Fluids **25**, 014103 (2013); 10.1063/1.4774321

Fiber-optic sensor system for heat-flux measurement
Rev. Sci. Instrum. **75**, 1006 (2004); 10.1063/1.1646768

Optical fiber refractometer
Rev. Sci. Instrum. **58**, 2047 (1987); 10.1063/1.1139513

Measurement of salinity distributions in salt-stratified, double-diffusive systems by optical deflectometry
Rev. Sci. Instrum. **57**, 2538 (1986); 10.1063/1.1139107

Accurate phase-measurement system for fiber-optic accoustic sensor
J. Acoust. Soc. Am. **68**, S95 (1980); 10.1121/1.2005016

This article is copyrighted as indicated in the article. Reuse of AIP content is subject to the terms at: http://scitationnew.aip.org/termsconditions. Downloaded to IP: 129.237.46.99 On: Thu, 12 Nov 2015 15:08:15

Miniature fiber-optic refractometer for measurement of salinity in double-diffusive thermohaline systems

T. L. Bergman,[a] F. P. Incropera,[a] and W. H. Stevenson[b]

School of Mechanical Engineering, Purdue University, West Lafayette, Indiana 47907

(Received 7 September 1984; accepted for publication 9 October 1984)

Information on salinity and temperature distributions is important in the study of thermohaline systems. In order to overcome difficulties associated with existing measurement methods, a miniature fiber-optic probe has been developed. The probe, which is capable of local quasisteady and fluctuating salinity and temperature measurements, is easily constructed, calibrated, and utilized. Probe measurements compare favorably with results obtained using a slant-wire shadowgraph technique and clearly show local phenomena in double-diffusive thermohaline systems.

INTRODUCTION

Recent interest in double-diffusive convection processes occurring in geophysical and engineering thermohaline systems, such as the ocean[1] and the salt-gradient solar pond,[2] has prompted the development of instrumentation for simultaneously measuring local salinity and temperature. To date, emphasis has been placed on the development of electroconductivity probes,[3] although optical methods, such as Mach–Zehnder interferometry,[4] have also been considered. Unfortunately, such methods are characterized by many difficulties.

Electrode erosion and/or corrosion is a major problem associated with electroconductivity probes in the salty environment of thermohaline systems. Due to changing electrode surface conditions, probe output is subject to considerable drift and periodic recalibration, often *in situ*, is required.[5,6] Calibration is complicated by the highly nonlinear dependence of conductivity on salinity,[7] which causes probe sensitivity to be strongly influenced by the salinity of the sampled solution. Recalibration difficulties due to corrosion/erosion of the probe surface may be minimized by using larger probes, but only at the expense of decreased spatial resolution and, in some cases, increased time response.[8] Stray currents between the electroconductivity probe and the surrounding test cell or "cross talk" between multiple probes[9] may also result in spurious output. Finally, the need to use precious metals, such as platinum[3,5,6,8,9] for probe components can result in a high cost of construction.

Since the refractive index of a salt solution depends on salinity and temperature, optical techniques such as Mach–Zehnder interferometery have been used to measure salinity in thermohaline systems.[4] However, such techniques are limited by the ability to resolve the closely spaced fringes associated with large refractive index gradients,[4] by the need to spatially average along the test beam,[10] and by refraction errors associated with beam deflection in large refractive index gradients.[11] Also, due to spatial averaging, the method may not be used in convectively mixed fluid regions, which are not characterized by well-defined fringe patterns.

Despite limitations associated with spatially averaging optical techniques such as Mach–Zehnder interferometry, the fact that the index of refraction varies with the salinity and temperature of a thermohaline system suggests that measurement of the local refractive index and temperature may be used to accurately infer the local salinity. For example, the refractive index of a thermohaline system may be determined by measuring the angle of deflection of a laser beam as it traverses a glass–thermohaline solution interface and subsequently employing Snell's law. This concept has been used in the design of a submersible point refractometer for oceanic measurements.[12] However, the large size of the instrument (≈ 1.0 m long by 0.1 m in diameter) precludes its use for laboratory experimentation.

While the angle of the refracted beam at an interface between glass and a thermohaline solution depends on the ratio of refractive indices n_g/n_s, the amount of light transmitted through the interface also varies with n_g/n_s as described by the Fresnel equations.[13] For an internal reflection ($n_g/n_s > 1$) and a constant angle of incidence, the amount of light transmitted through the interface increases (or decreases) as n_g/n_s decreases (or increases). Hence, measurement of the amount of transmitted or reflected light may be used to determine n_g/n_s.

Miniaturization of a probe designed to detect changes in the amount of light transmitted through a glass–water interface has been accomplished by utilizing optical fiber with a U-shaped microbend as the refracting surface.[14] The experimental apparatus consisted of a light source, fiber-optic probe, and detection device shown schematically in Fig. 1. Losses from the fiber to the surrounding fluid vary with the refractive index of fluid adjoining the U bend, leading to a variation in the energy input to, and hence the output signal from, the detection device. The probe was not used to monitor continuous variations in the refractive index of the fluid; rather it was utilized in a binary (on–off) fashion to detect the presence of vapor bubbles in a two-phase system. Subsequent investigation of this miniature fiber-optic refractometer concept[15] has, however, suggested that it may have sufficient sensitivity to be calibrated and used to detect small variations in the fluid refractive index. Hence, in view of the many difficulties associated with using electroconductivity probes, the purpose of this study was to construct and calibrate a miniature fiber-optic refractometer and to demon-

 0034-6748/85/020291-06$01.30 © 1985 American Institute of Physics

This article is copyrighted as indicated in the article. Reuse of AIP content is subject to the terms at: http://scitationnew.aip.org/termsconditions. Downloaded to IP: 129.237.46.99 On: Thu, 12 Nov 2015 15:08:15

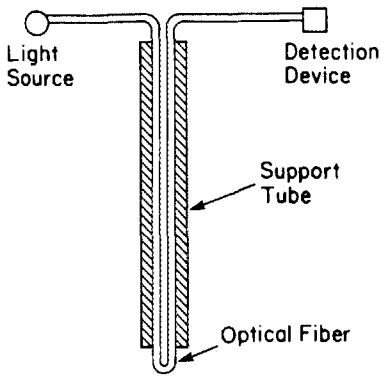

FIG. 1. Miniature fiber-optic refractometer (Ref. 14).

strate its applicability to point temperature and salinity measurements in a thermohaline system.

I. PROBE DESIGN

The refractive index of thermohaline solutions depends on both temperature and salinity. As such, to determine the salinity, a local temperature measurement must be performed in conjuction with measurement of the local refractive index. Knowing the local temperature and salinity, other thermophysical properties such as the local density may be determined from accepted polynomial fits of existing data for thermohaline systems.[16]

The bent fiber-optic refractometer concept was used in this study. A 0.4-mm-diam fiber, consisting of a 0.372-mm-diam polystyrene core with 0.014-mm-thick methyl methacrylate cladding and rubber coating, was inserted in a 3-mm-diam stainless-steel support tube as shown in Fig. 2. The cladding and coating were selectively removed from the U bend by lightly sanding a flat surface on the fiber optic, allowing intimate contact between the polystyrene core and the thermohaline solution. The thermocouple bead (3 mil, copper constantan) was positioned in the x, y plane approximately 1 mm from the optical fiber. The thermocouple leads were also inserted in the stainless-steel tubing and the entire probe tip assembly was sealed with epoxy (3M, Scotch-Weld Structural Adhesive). A photograph of the probe tip is provided in Fig. 3.

Although further probe miniaturization may be effected by mounting the optical fiber in a smaller diameter support tube, the reduced radius of the U bend would substantially increase light loss from the probe tip, thereby

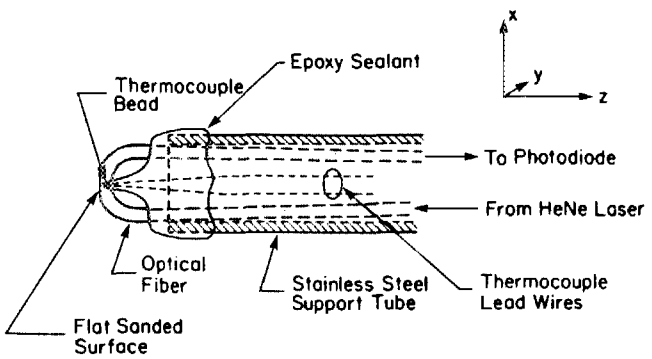

FIG. 2. Schematic of the fiber-optic refractometer probe tip.

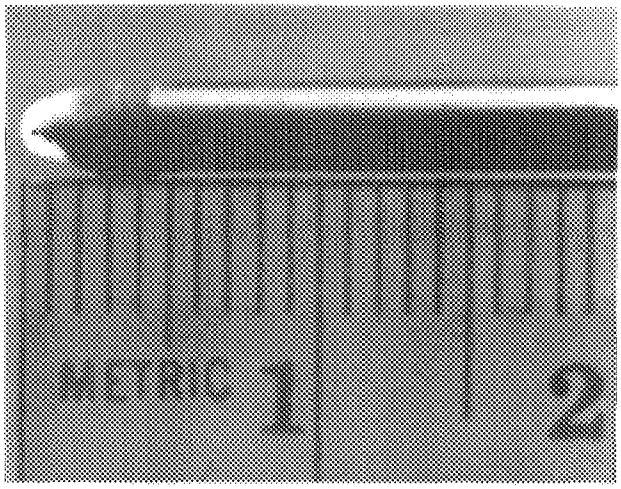

FIG. 3. Photograph of the fiber-optic refractometer probe tip (scale in centimeters).

decreasing the output signal level. As such, selection of the support tube diameter is a trial-and-error procedure to achieve a suitable trade-off between probe miniaturization and signal quality. The optimum U-bend radius, and thus support tube diameter, depends on the fiber material and the desired spatial resolution.

A schematic of the complete electrical–optical system is shown in Fig. 4. Illumination of the fiber optic is provided by a 5-mW helium–neon laser. The attenuated output of the fiber-optic probe, which is mounted on a vertical transversing device, is converted to a current signal by a United Detector Technology PIN-100F photodiode. The output of the photodiode is subsequently sent to an I/V transformer (Keithly 18 000-20) whose filtered voltage output is monitored by a Hewlett–Packard 3054A data-acquisition system. The location of the probe tip, which is obtained with a precision linear potentiometer attached to the traversing mechanism, and the temperature are also monitored with the data-acquisition system.

II. PROBE CALIBRATION

Light transmission through the core of an optical fiber in the vicinity of a microbend (small U bend) depends on the ratio of the refractive indices of cladding and core. By selectively removing the cladding from the bend, thermohaline solution is brought into contact with the core. Hence, variations in the refractive index of the thermohaline solution will

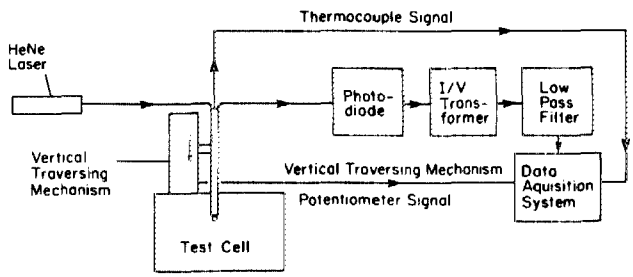

FIG. 4. Schematic of experimental apparatus.

This article is copyrighted as indicated in the article. Reuse of AIP content is subject to the terms at: http://scitationnew.aip.org/termsconditions. Downloaded to IP: 129.237.46.99 On: Thu, 12 Nov 2015 15:08:15

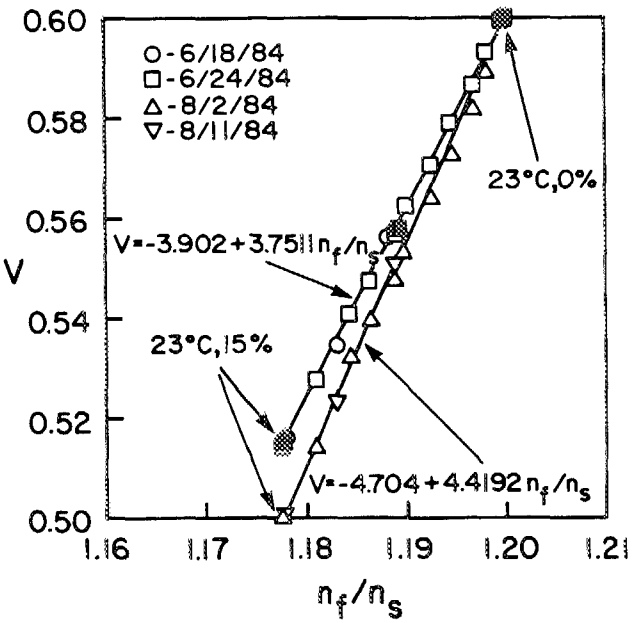

FIG. 5. Calibration of the fiber-optic refractometer.

alter the amount of light transmitted through the microbend and detected by the photodiode. Thus, the output voltage of the I/V transformer may be calibrated as a function of the ratio of the fiber-optic refractive index to the solution refractive index η_f/η_s. Calibration data were obtained and the results are shown in Fig. 5. Since the refractive index of a thermohaline solution varies with both temperature and salinity, the ratio n_f/n_s may be varied by changing either parameter in a saltwater sample. The open data symbols of Fig. 5 correspond to calibrations performed at room temperature (23 °C) with samples of various salinity (0%–15%), as determined by a weight analysis. Solid data symbols were obtained by heating various constant salinity samples to approximately 33 °C. In this case consideration must be given to the fact that the refractive index of the polystyrene fiber also varies with temperature. The temperature dependence of n_s is obtained from polynomial curve fits developed for thermohaline solutions,[16] while the temperature dependence of n_f is calculated from[17]

$$n_f = 1.60\text{–}1.65\times 10^{-4}(T-20), \tag{1}$$

where T is the sample temperature (°C).

The miniature fiber-optic refractometer was calibrated four times, and, as shown in Fig. 5, only a slight shift occurred over a 2-month interval. The shift may be due to slight changes in the geometry of the U bend, as the first two calibrations were performed shortly after probe construction. Note that increased probe sensitivity resulted from the calibration shift.

Due to alignment variations of the optical equipment, the position of the laser was adjusted prior to each calibration with the probe submersed in pure water at 23 °C until the output signal was 0.60 V. Since polystyrene slowly absorbs water,[18] the probe was stored in fresh water between calibration, in order to avoid transient absorption-induced calibration error. In addition, it was necessary to allow the electrooptical system to reach steady-state thermal conditions ($\approx$6h) before each calibration could be performed.

The calibration curves are nearly linear throughout the entire range of salinities (0%–15%) and temperatures (23°–33 °C), which suggests that probe sensitivity is nearly independent of temperature and salinity. Also, the output voltage is much more sensitive to salinity variations than to temperature variations

$$\left(\frac{\partial V}{\partial m_s}|_T\right)dm_s \rangle\rangle \left(\frac{\partial V}{\partial T}|_{ms}\right)dT, \tag{2}$$

where dm_s and dT are the salinity and temperature ranges normally encountered, suggesting that extremely accurate measurement of the local temperature is not essential for systems characterized by large salinity variations.

Since the output signal of the fiber-optic refractometer is a dc voltage, fluctuating salinity, as well as temperature measurements may be made. Evaluation of the time constant of the fiber-optic device is limited by the relatively slow response of the associated electronics and was estimated to be less than 1 ms by recording the output signal on a storage oscilloscope while transferring the probe from air to a water solution. The thermocouple time constant was similarly determined and its much larger value (70 ms) is due to the thermal capacitance of the epoxy coating, which was applied to the thermocouple bead for corrosion protection. Both time constants could be reduced if necessary by appropriate design changes.

Neglecting any influence of the solution refractive index on net light loss from the core into the methyl methacrylate cladding, the spatial resolution of the probe corresponds to the volume occupied by the sanded portion of the probe tip; or approximately $1.0\times 0.1\times 0.0$ mm in the x, y, and z directions, respectively. Application of an opaque material such as an epoxy to the clad portion of the optical fiber, may easily be performed in order to ensure isolation of the fiber from the thermohaline solution and hence a vertical spatial resolution of zero.

III. UTILIZATION OF THE FIBER-OPTIC PROBE IN DOUBLE-DIFFUSIVE THERMOHALINE EXPERIMENTATION

To test the fiber-optic probe, an experiment was performed in which a salt-stratified solution was first established and then destabilized by an applied bottom heat flux. Experimentation was performed in a test cell with a square base ($305\times 305\times 200$ mm) and 25-mm-thick acrylic side walls. The base consisted of an electronic patch heater sandwiched between a 1.6-mm copper plate, which served as the bottom of the test cell, and a 25-mm sheet of styrofoam. The walls of the test cell were insulated with 50-mm styrofoam sheets. The fiber-optic probe was attached to a vertical traversing mechanism which was mounted above the test cell and was used to collect data at 5-s intervals while traversing the solution at a speed of 0.76 mm/s. A laser illuminated shadowgraph was also used to monitor conditions within the thermohaline solution.

Three phases of experimentation were considered and included: (i) use of the fiber-optic refractometer to monitor salt diffusion in an isothermal, salt-stratified solution, (ii) use of the probe to measure salinity and temperature profiles in a

This article is copyrighted as indicated in the article. Reuse of AIP content is subject to the terms at: http://scitationnew.aip.org/termsconditions. Downloaded to IP: 129.237.46.99 On: Thu, 12 Nov 2015 15:08:15

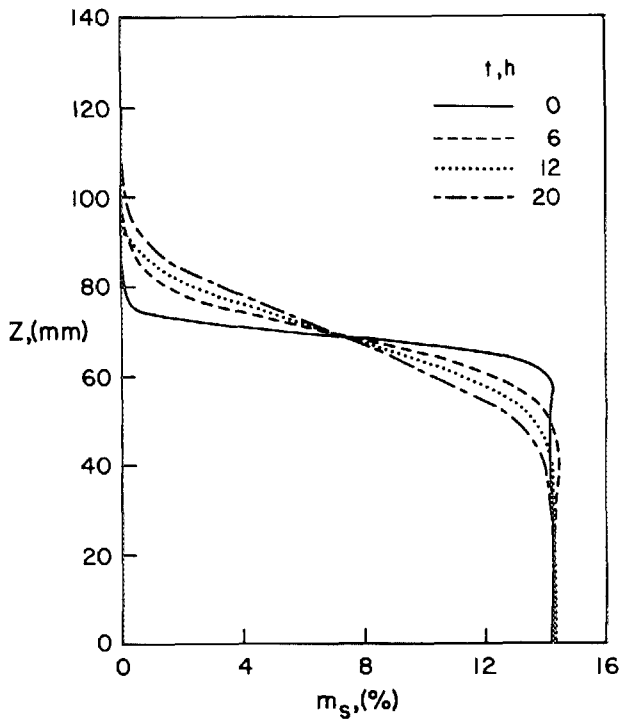

FIG. 6. Transient salinity profiles in an isothermal system as measured by the fiber-optic refractometer.

salt-stratified solution heated from below, and (iii) use of the probe to measure fluctuating temperatures and salinities in a heated solution.

In the first experimental phase, the test cell was filled to a height of 140 mm with two 70-mm-deep layers of uniform salinity (0% and 14.5%). The top of the test cell was covered with an acrylic panel to minimize evaporative heat loss from the air–water interface and the solution was allowed to diffuse for 26 h. The diffusion process was monitored by traversing the fiber-optic probe and representative results are shown in Fig. 6.

The salinity distribution, which is approximately a step function at $t = 0$ h (some mixing of the two fluid layers occurs during the filling process accounting for variations in the profile near $Z = 70$ mm), assumes the form of a smooth profile with increasing time to $t = 20$ h. Diffusion effects propagate upward and downward from $Z = 70$ mm, while the average salinity gradient at $Z = 70$ mm decreases with time.

Characteristics of the diffusing salinity distributions shown in Fig. 6 are also revealed by the shadowgraphs of Fig. 7. When a slanted wire is placed in the shadowgraph beam in front of the test cell prior to filling, its shadow propagates directly to a screen placed against the opposite test cell wall [$t < 0$ h, Fig. 7(a)]. After the two fluid layers are introduced, however, the shadow of the slanted wire is deflected downward by the large salinity (and, hence, refractive index) gradient centered at $Z = 70$ mm [$t = 0$ h, Fig. 7(b)]. Deviation of the deflected shadow from the location of the wire ($Z = 57$ and 78 mm) indicates the extent of vertical propagation from the interface at $Z = 70$ mm due to mixing effects.[19] At $t = 12$ h [Fig. 7(c)], the salinity gradient at $Z = 70$ mm has been considerably reduced while the salinity profile has propagated to $Z = 38$ and 100 mm. Extension of the salinity profile to

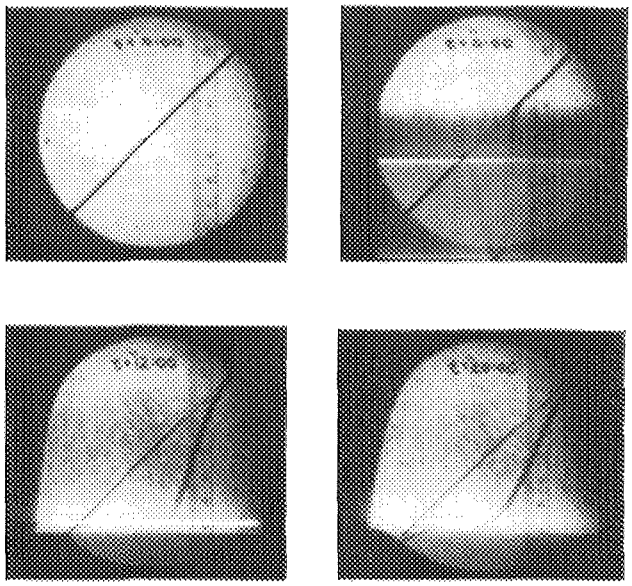

FIG. 7. Shadowgraphs of the transient conditions of Fig. 6 for (a) $t < 0$ h, (b) $= 0$ h, (c) $t = 12$ h, (d) $t = 20$ h.

these limits is in good agreement with the measured profile of Fig. 6. At $t = 20$ h [Fig. 7(d)], the salinity gradient has been further reduced and the height of the diffusion zone has exceeded the view of the shadowgraph.

To test the effectiveness of the probe in measuring salinities and temperatures under double-diffusive conditions, the salt-stratified isothermal solution at $t = 26$ h (Fig. 8) was destabilized by an applied bottom heat flux of 500 W/m^2. In such systems, convection is confined to a mixed layer which is characterized by uniform salinity and temperature distributions and is adjacent to the heating surface. The mixed

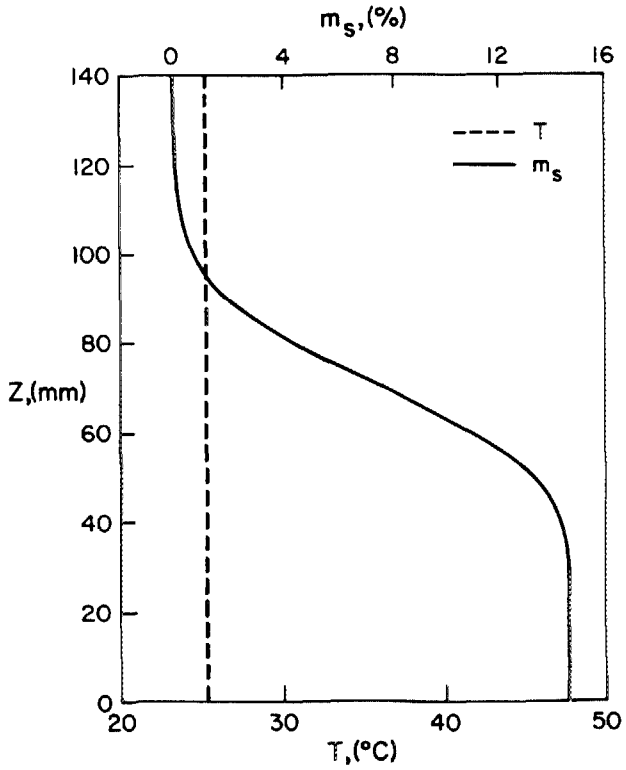

FIG. 8. Measured salinity and temperature profiles at $t = 26$ h.

This article is copyrighted as indicated in the article. Reuse of AIP content is subject to the terms at: http://scitationnew.aip.org/termsconditions. Downloaded to IP: 129.237.46.99 On: Thu, 12 Nov 2015 15:08:15

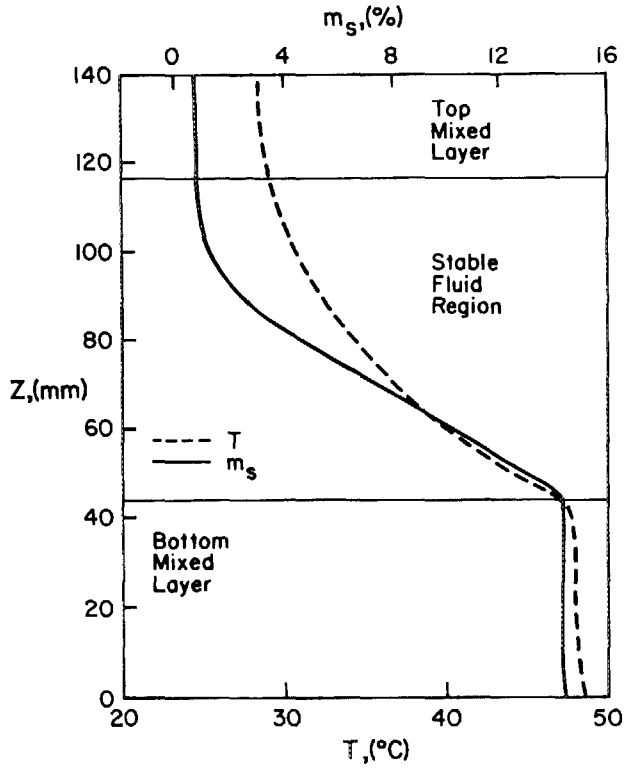

FIG. 9. Measured salinity and temperature profiles at $t = 31$ h.

layer grows slowly at the expense of overlying stable fluid, while acting as a heat source for the remainder of the system. The final temperature and salinity profiles ($t = 31$ h) are shown in Fig. 9. A mixed layer of height $\delta = 42$ mm is clearly denoted by the existence of uniform salinity and temperature profiles below this location. In addition, there is evidence of a top mixed layer which is driven by heat transfer from the stable region to the top layer and heat losses from the air–water interface. The entrainment of stable fluid into the top mixed layer has caused the salinity at the air–water interface to increase above its initial value of zero. It should be noted that expressions for n_s^{16} have been extrapolated for situations where $T > 40$ °C.

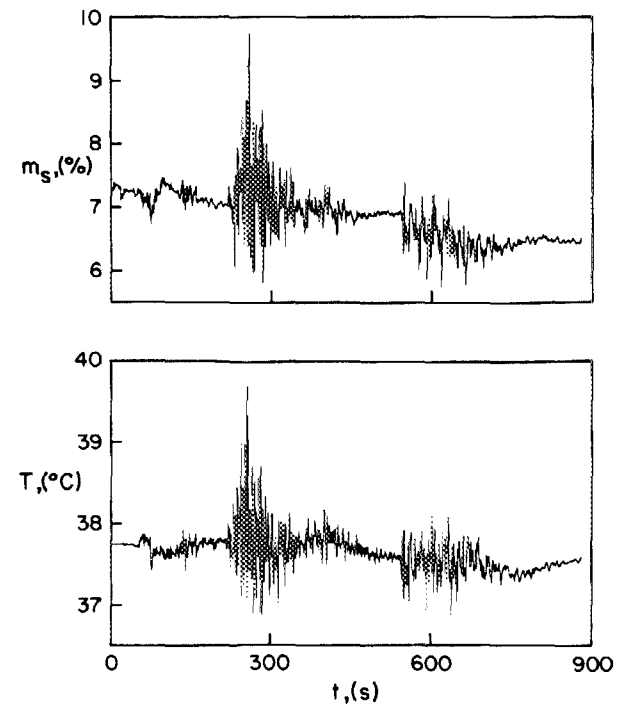

FIG. 10. Measured fluctuating salinity and temperature histories.

The results of Figs. 6–9 demonstrate that the miniature fiber-optic probe can be used to measure quasisteady salinities in isothermal systems and both salinities and temperatures in a double diffusive, thermohaline system.

In the third phase of the experimentation, the probe was used to measure fluctuating salinities and temperatures. Since both salinity and temperature increase with depth in the stable fluid region of Fig. 9, any system disturbance which initiates gravity waves will result in temperature and salinity fluctuations at any location in the stable fluid. Furthermore, the gravity wave-induced fluctuations will be positively correlated, since any parcel of fluid possessing a higher (or lower) temperature will also be characterized by a larger (or smaller) salt content.

Figure 10 shows fluctuating temperature and salinity histories induced by tilting the test cell and measured by the fiber-optic probe. The probe was positioned at $z = 70$ mm in the stable region of Fig. 9. Data were sampled at 1-s intervals as the test cell was tilted at $t \approx 200$ and 550 s. As is evident, large spikes in the temperature history coincide with similar perturbations in the salinity record. A double correlation coefficient may be defined as

$$L = \overline{\Delta T \Delta m_s} / \overline{|\Delta T \Delta m_s|}, \tag{3}$$

where ΔT and Δm_s are temperature and salinity fluctuations

$$\Delta T = T - \bar{T}, \tag{4a}$$

$$\Delta m_s = m_s - \bar{m}_s, \tag{4b}$$

and the overbars denote average temperature or salinity

$$\bar{T} = \frac{1}{N} \sum_{n=1}^{N} T, \tag{5a}$$

$$\bar{m}_s = \frac{1}{N} \sum_{n=1}^{N} m_s, \tag{5b}$$

for a total of N sample measurements. The value of L for the data of Fig. 10 is 0.923, which deviates slightly from the ideal value of $L = 1.0$ corresponding to an exact correlation of the two fluctuations. This deviation from the ideal value may be due to different diffusion rates for salt and heat and to different time constants associated with the fiber-optic probe and the thermocouple. Nevertheless, the good agreement between measured and ideal values of L suggests that the miniature fiber-optic refractometer is well suited for monitoring temperature and salinity fluctuations in thermohaline systems.

ACKNOWLEDGMENTS

Support of this work by the National Science Foundation under Grant No. MEA-8316580 is gratefully acknowledged. Useful suggestions by Tom Pack and Hans Bukow are appreciated.

This article is copyrighted as indicated in the article. Reuse of AIP content is subject to the terms at: http://scitationnew.aip.org/termsconditions. Downloaded to IP: 129.237.46.99 On: Thu, 12 Nov 2015 15:08:15

[a] Heat Transfer Laboratory.
[b] Applied Optics Laboratory.
[1]J. S. Turner, *Buoyancy Effects in Fluids* (University of Cambridge, Cambridge, 1979).
[2]H. Tabor, Solar Energy **27,** 181 (1981).
[3]S. Thangam and C. F. Chen, Geophys. Astrophys. Fluid Dynamics **18,** 111 (1981).
[4]W. T. Lewis, F. P. Incropera, and R. Viskanta, J. Fluid Mech. **116,** 411 (1982).
[5]T. B. Meagher, A. M. Pederson, and M. C. Gregg, in the Oceans 82 Conference Record, Washington, DC (IEEE, New York, 1982), p. 283.
[6]D. P. Grimmer, G. F. Jones, J. Tafoya, and T. J. Fitzgerald, Rev. Sci. Instrum. **54,** 1744 (1983).
[7]U. S. Office of Saline Water, *Technical Data Book* (United States Department of the Interior, 1964).
[8]M. J. Head, Ph. D. thesis, University of California, San Diego, 1983.
[9]S. J. Khang and T. S. Fitzgerald, Ind. Eng. Chem. Fundam. **14,** 208 (1975).
[10]W. Hauf and U. Grigull, in *Advances in Heat Transfer,* edited by T. F. Irvine and J. P. Hartnett (Academic, New York, 1970), Vol. 6, p. 133.
[11]V. Sernas, in *Proceedings of the Third International Symposium on Flow Visualization* (Hemisphere, Washington, 1983), p. 428.
[12]K. H. Mahrt, H. C. Waldermann, and W. Kroebel, in the Oceans 82 Conference Record, Washington, DC (IEEE, New York, 1982), p. 266.
[13]E. Hecht and A. Zajac, *Optics* (Addison–Wesley, Reading, MA, 1979), p. 72.
[14]J. M. Delhaye, M. Giot, and M. L. Riethmuller, in *Thermohydraulics of Two-Phase Systems for Industrial Design and Nuclear Engineering* (Hemisphere, Washington, 1981), p. 86.
[15]T. Takeo and H. Hattori, Jpn. J. Appl. Phys. **21,** 1509 (1982).
[16]B. R. Ruddick and T. G. L. Shirtcliffe, Deep Sea Res. **26,** 775 (1979).
[17]R. H. Wiley and G. M. Braur, J. Polymer Sci. **3,** 455 (1948).
[18]1980 *Materials Selector,* edited by R. Stedfeld *et al.* (Penton/IPC, Cleveland, 1980), p. C118.
[19]D. E. Mowbray, J. Fluid Mech. **27,** 595 (1967).

This article is copyrighted as indicated in the article. Reuse of AIP content is subject to the terms at: http://scitationnew.aip.org/termsconditions. Downloaded to IP: 129.237.46.99 On: Thu, 12 Nov 2015 15:08:15